Chapter 6

Cl_2 in Ar

6.1 DIM-Potentials and Interactions

The potentials of Cl_2 in Argon were calculated using the DIM approach discussed in chapter 4. First, all the different pair interactions have to be determined and from this the total system Hamiltonian is built:

$$\hat{H}_{total} = \underbrace{H_{mol}^{Cl_2} + V_{SO}^{Cl_2}}_{Cl_2} + \underbrace{\sum_X \sum_k U_{X,k}^{DIM}(r_{X,k}, \gamma_{Cl,k})}_{Cl-Ar} + \underbrace{\sum_{k,l} V_{Ar_k - Ar_l}}_{Ar-Ar} \tag{6.1}$$

The Valence-Bond basis set for Cl_2 consists of 36 states, as described in Section 4.2 for ClF. Both of the chlorine atoms have $1s^2 2s^2 2p^6 3s^2 3p^5$ configuration. Again only the valence electrons are taken into account and the electron hole is treated like in section 4.4.2, changing the sign of spin-orbit interaction terms.
For the molecular part in equation 6.1 ab initio calculations of gas phase potentials for Cl_2 by Kokh [47] without spin-orbit coupling were used. These potentials were associated with their appropriate valence bond wavefunctions and establish the diagonal elements of the system Hamiltonian $H_{mol}^{Cl_2}$ like discussed in chapter 4.1. See (Fig. 6.4, label a)). The ground state has a minimum of 2.49 eV. Only one of the other states is bound, namely the $^3\Pi$ state with a dissociation energy of 0.23 eV.
To this the spin-orbit coupling elements $V_{SO}^{Cl_2}$ calculated in chapter 4.4 are added, using l,s-coupling for the separated chlorine atoms [49, 48]. Again the spin-orbit

coupling is assumed to be constant and independent on the distance between the chlorine atoms.

Interaction with the rare gas atoms is included isotropically and anisotropically

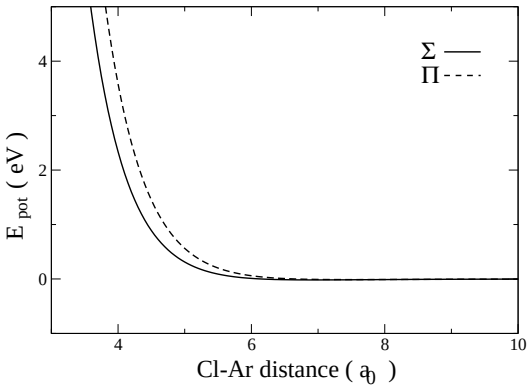

Figure 6.1: *Cl-Ar interaction:* Σ *and* Π *potentials [51]*

as described in section 4.3. The potentials were determined by Aquilanti et al. in crossed molecular beam studies of Ar scattering from Cl(^2P) [51]. Potentials are depicted in Fig. 6.1. The Σ state shows a very shallow minimum at 6.5 a_0 and a strong repulsion at shorter distances.

The pair potentials between the argon atoms (see chapter 4 and equation 6.1) are taken from Aziz and Slaman [50].

At each timestep all these interactions are added to the Hamiltonian. Subsequent diagonalization will result in the adiabatic potentials, as described in section 2.

6.2 Ground State Geometry

Argon crystallizes in an face centered cubic lattice according to space group Fm3-m and cell parameters a=b=c= 10.042 a_0, $\alpha = \beta = \gamma = 90°$. Because of the similarity of the van-der-Waals radii of chlorine (1.75 Å) and argon (1.88 Å) and the diameter of 3.755 Å for one substitutional site the chlorine molecule is considerably too large to occupy only a single substitutional site. This has been confirmed by calculations with one or two of the argon atoms in the matrix replaced by the chlorine molecule and to find the optimal geometry the system was cooled down with long time of relaxation (> 1 ps). As expected the disubstitutional site gave the optimal geometry, including small displacements in the surrounding argon atoms.

Fig. 6.2 shows the site and orientation of the chlorine molecule in the argon lattice. Two neighbouring argon atoms have been replaced by the chlorine atoms.

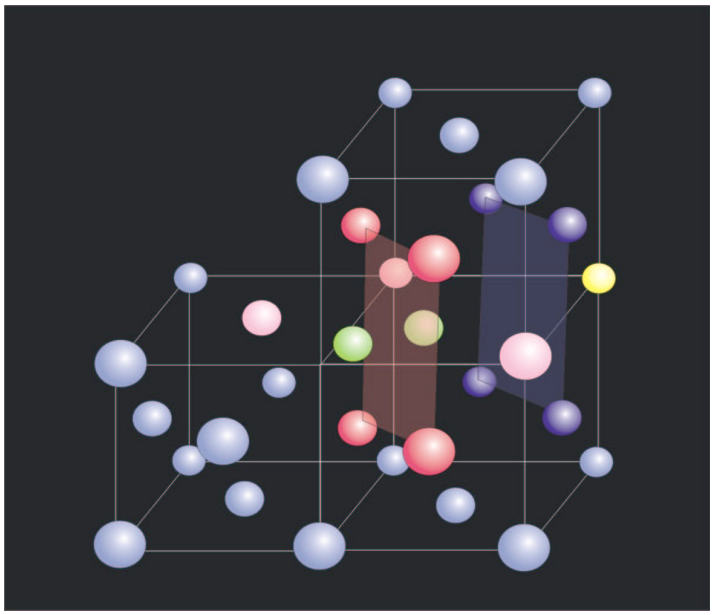

Figure 6.2: *Orientation and site of a chlorine molecule embedded in an argon matrix, red: belt atoms, yellow: collision atom, blue: window atoms, pink: phonon atoms*

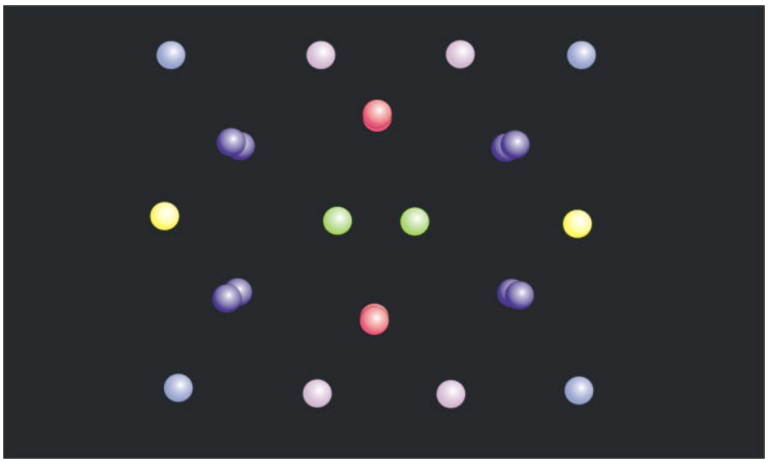

Figure 6.3: *Orientation and site of a chlorine molecule embedded in an argon matrix, view from above*

First, the most important argon atoms in the vicinity of the impurity have to be

identified: As can be seen from Fig. 6.2 and from Fig. 6.3, there are four atoms (in red) lying around the center of the Cl-Cl bond and will be therefore called *belt* atoms. As can easily be seen from Fig. 6.2 they are located in the layers above and below the chlorine molecule. The next group of argon atoms are the two argon atoms lying in the direction of the axis of the impurity molecule, which play an important role in the dynamics. These are called *collision* atoms (yellow). The next group consists of eight atoms, four in the direction of each chlorine atom respectively. Like the belt atoms they are located in layers above and below the layer which holds the chlorine molecule and are called *window* atoms (blue). The last group are the nearest neighbours of the chlorine molecule in the same layer, which span a rectangle (only three of them are shown in Fig. 6.2) and they can best be seen in Fig. 6.3. Their role in the course of the dynamics is supposed to be connected to phonon modes which are impulsively excited, as described in section 1.4.2, so they will be called *phonon* atoms (pink). Since the chlorine molecule exhibits a shorter bond length than the argon-argon distance in the lattice (1.98 Å for Cl-Cl versus 3.7 Å for Ar-Ar), the nearest neighbours are slightly displaced (Fig 6.3). The most distinct effect is the one on the belt atoms, which will be pushed outwards due to the repulsion resulting from the smaller distance to the chlorine molecule. On the other hand the window atoms will have more space left and shift slightly inwards. Phonon and collision atoms are not shifted significantly.

6.3 Potentials for Cl_2 in Ar

After diagonalization of the Hamiltonian, the resulting eigenenergies of the system can be seen in Fig. 6.4. The potentials were calculated (panel b) and c)) by fixing all of the argon atoms at their initial positions and elongating the Cl-Cl distance, representing a cut through the potential energy surface. It has to be emphasized that these cuts do not represent the effective potentials during the simulations, because at each time step the potential energy of the system will be recalculated, including the atomic displacements of all the atoms.

The general effects on the gas phase potentials can be described as follows: First, including the spin-orbit coupling in the calculation leads to a splitting of degenerate levels, which can be clearly seen for the lowest lying triplet states ($^3\Pi$) in Fig. 6.4, label b). The second effect is due to the matrix, resulting in the caging of the molecule when the chlorine atoms reach the vicinity of the next argon atoms. Here the potential becomes repulsive and in the Franck-Condon

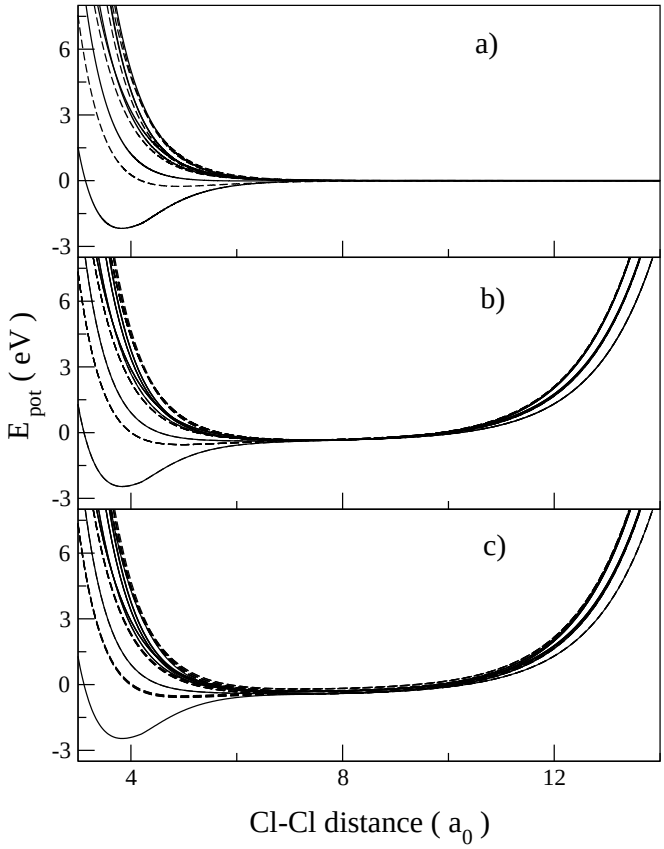

Figure 6.4: *1d-potentials of Cl_2: a) gas phase, b) in Ar, without spin-orbit coupling, c) in Ar, including spin-orbit coupling. Solid lines are assigned to singlet states, dashed lines to triplet states*

region the excess energy of the atoms after photoexcitation will not be sufficient to overcome this barrier. Taking into account the motion of the collision atoms in the direction of the molecular bond will lead to 2d-potentials as shown in Fig. 6.8.

6.3.1 Matrix Shift

By embedding a molecule in a matrix environment its energy levels are affected. There are two important contributions to that, first the so called solid shift $\delta\omega_S = \omega_S - \omega_{gas}$ [54]. This can be seen in the shifting of the minimum of the ground state of the molecule to lower energy. The second is the relative shift of the vibrational frequencies $\delta\omega/\omega$, which is due to some deformation of the gas phase potential of a molecule when embedded in a matrix. The effect for Cl_2 can be seen in Fig. 6.5. The matrix embedded potential is shifted to lower energy, while the potential

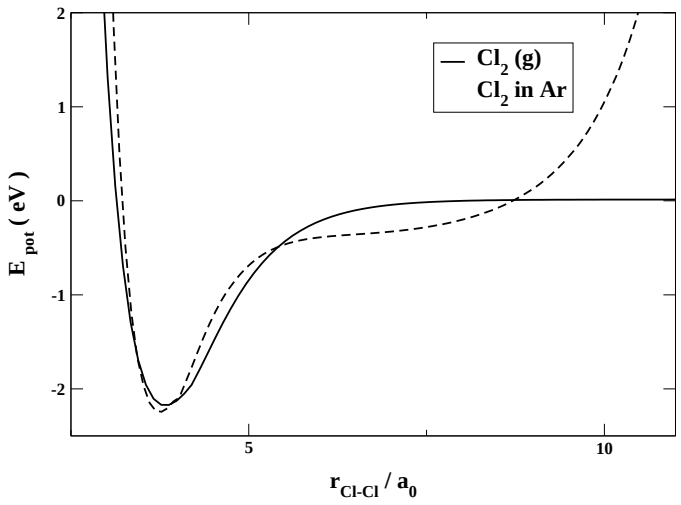

Figure 6.5: *Ground state potential of Cl_2 in gas phase and embedded in Ar*

gets steeper. This will result in a shifting of the vibrational frequencies. ω equals 564.9 cm^{-1} in the ground state [87] for the gas phase and 578.6 cm^{-1} for the matrix embedded species. The relative shift has a value of 2.4 % and this is in good agreement with the experimentally observed shifts as referred in [52].

6.4 Assignment of Electronic States

By diagonalizing the matrix with all interactions included, 36 eigenvalues for each time step are evaluated which belong to the different adiabatic states for the system embedded in the matrix.

$$H_{total}|\Phi_\lambda(t)\rangle = V_{\lambda,adiab.}(t)|\Phi_\lambda(t) \tag{6.2}$$

At the ground state equilibrium distance the main character of the lowest adiabatic states can be assigned to a pure state of the chlorine molecule. Three groups which show a significant influence on the dynamics can be identified: State number zero belongs to the ground $X\,^1\Sigma_g$ state of the molecule, which shows a potential minimum of 2.52 eV at 3.825 a_0. The states one to six can be assigned to the six different $^3\Pi_u$ states of the molecule. This number is due to the fact that we have two possible projections of the angular momentum vector (m_L = -1,1) and three different projections of the spin (m_S = -1,0,1). The most important one of these, the B$^3\Pi^+_{0u}$ state, which will be coupled to the degenerate C ($^1\Pi_u$)-states via spin-orbit coupling, has a potential minimum at 4.9 a_0. States seven and eight belong to the $^1\Pi_u$ with m_L=$\pm$1 or C-state of the chlorine, which will be initially excited. They show a very shallow minimum (approx. 0.4 eV) at r = 6.9 a_0. The degeneracy is lifted by the introduction of spin-orbit coupling (SOC). Here we take into account the energetically lowest one of these two states with projection m_L = 1. This state is coupled via SOC to one of the triplet states ($^3\Pi^+_{0u}$). The one-dimensional cut of the most important three potentials is given in Fig.6.6

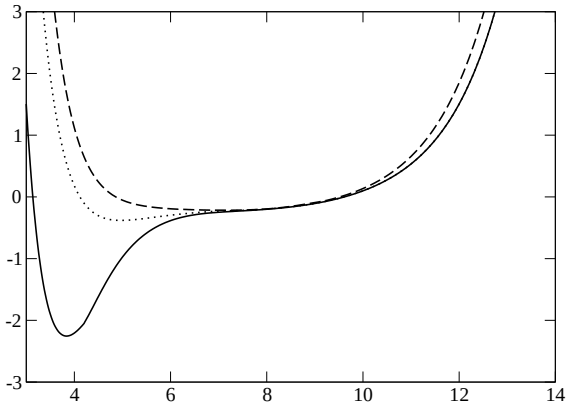

Figure 6.6: *Three important potentials for the course of the dynamics. Solid line : X- ($^1\Sigma^+_g$), dotted: B- ($^3\Pi_u$), dashed: C- ($^1\Pi_u$) state*

At larger distances the character of the initially excited state will change to a mixture of the pure states without dominant contribution from one particular state, so that here an assignment to the pure states of the chlorine molecule is not

reasonable in the limit of the adiabatic separation. In Table 6.4 different contributions of the 'pure' VB-states to the adiabatic potentials during propagation on the C-state are given.

distance r (a_0)	dominant contributions				
3.8	99.9 % $^1\Pi_u$				
4.0	99.7 % $^1\Pi_u$	0.15 %$^3\Pi_u$			
5.0	97.6 % $^1\Pi_u$	0.4 % $X^3\Sigma_u$	0.3 % $^3\Pi_u$		
5.8	87.8 % $^1\Pi_u$	2.4 % $X^3\Sigma_u$	4.1 % $^3\Pi_u$	1.0 % $^3\Pi_g$	1.0% $^3\Delta_u$
6.4	68.3 % $^1\Pi_u$	8.5 % $X^3\Sigma_u$	8.4 % $^3\Pi_u$	8.6 % $^3\Pi_g$	3.0 % $^3\Delta_u$
7.0	26.5 % $^1\Pi_u$	15.4 % $X^3\Sigma_u$	32.3 % $^3\Pi_u$	15.2 % $^3\Pi_g$	5.3 % $^3\Delta_u$

Table 6.1: *Contributions of the VB-states to the adiabatic state, which can be initially assigned to the $^1\Pi_u$ state during the dynamics after excitation to this state. Corresponding potential energies are shown in Fig. 6.7.*

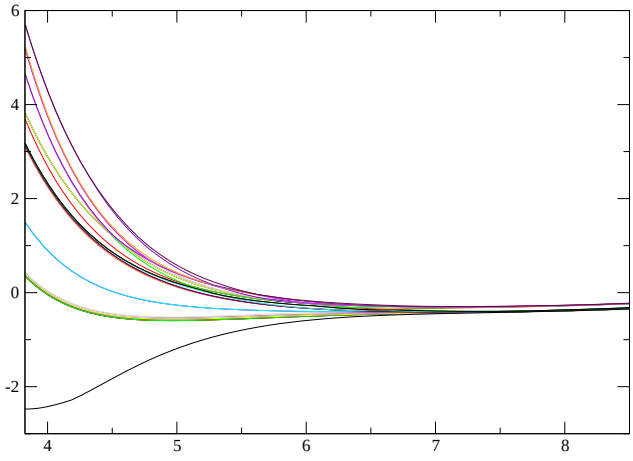

Figure 6.7: *Potential energies of the 36 adiabatic states of Cl_2 in Ar after excitation to the C-state along a trajectory.*

When the potentials come very close to each other, such as in Fig. 6.7, which shows all of the potentials after excitation of the C-state, the contributions will change significantly, reflecting the nearly degeneracy of the adiabatic states.

6.5 2d-Potential Surfaces

In order to study the interplay between Cl_2 and Ar motion in more detail, two-dimensional potential energy surfaces were calculated, taking into account the motion of chlorine and the motion of the collision atoms as a second degree of freedom. These are supposed to be the most significant in the course of the dynamics. All 36 2d-potential surfaces were calculated, the three most important are depicted in Fig. 6.8. The vertical line shows the coordinates after Franck-Condon excitation from the ground to the B and C state. Trajectories starting in either one of the states are expected to show a similar behaviour, except for the different magnitude of forces, potential and kinetic energy: The forces acting on the particles in both of the excited states will result in an elongation of the Cl-Cl bond. Reflection by the potential wall will then lead to enlargement of the Ar-Ar distance and a decrease of r_{Cl-Cl}. This may lead to recombination, but from these potentials there is no eye-catching path for the Cl atoms to leave the initial cage as in the case of ClF, which will be discussed in section 7.

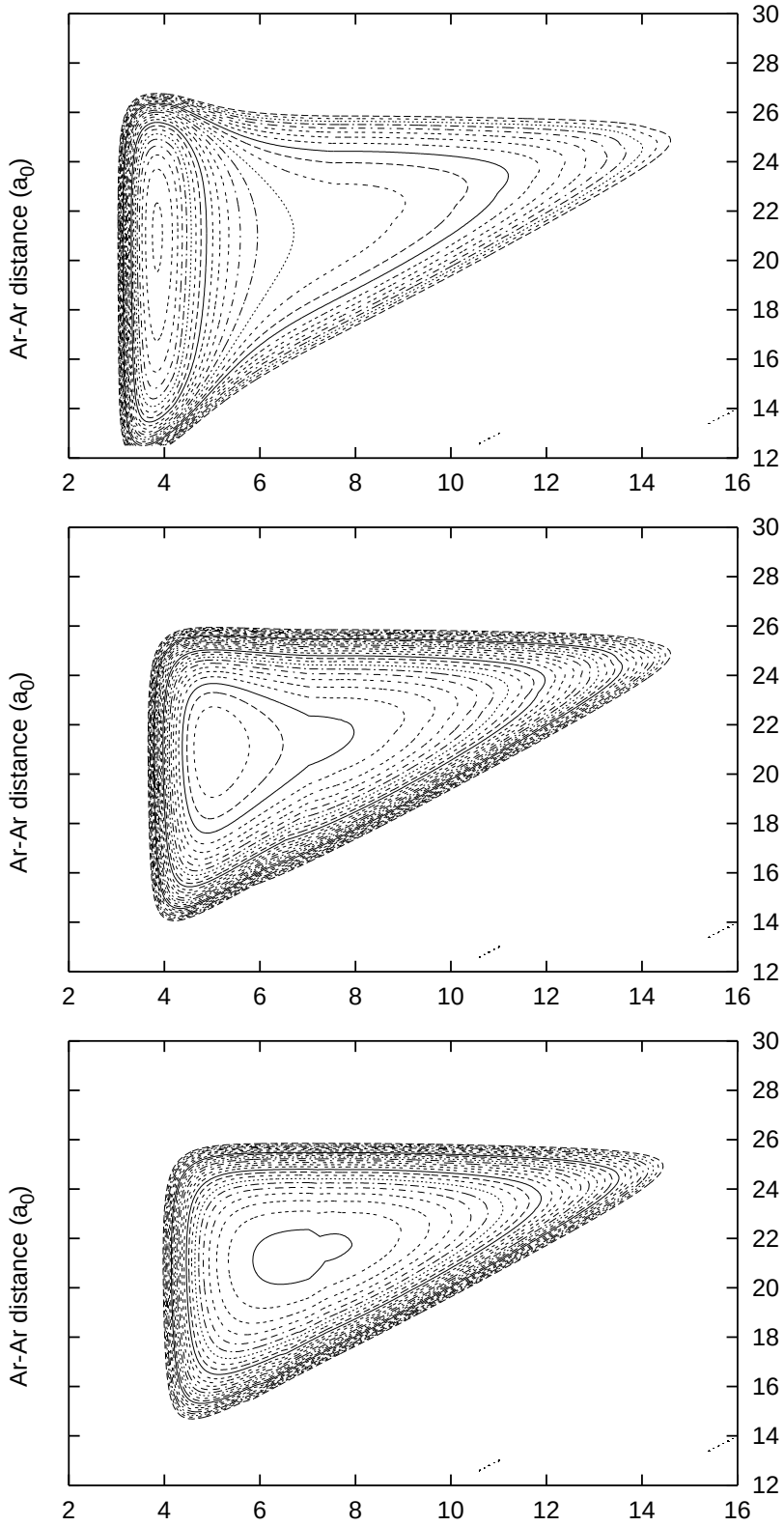

Figure 6.8: *Ground-, B- and C-state potentials of Cl_2 in Argon. Ordinate: collision atoms distance*

6.6 C-state Excitation

The first set of calculations was done to excitation to the C-state because it will be the energetically lowest state reachable with spin-allowed transition.
The calculations were performed with a chlorine molecule embedded in a matrix of 1272 argon atoms, meaning six unit cells in each direction. The excitation energy for the C-state is 3.98 eV. The potential surface is repulsive and so the chlorine molecule rapidly starts to dissociate. The excess energy of the chlorine will lead of a kinetic energy of 0.94 eV for each chlorine atom and a fast elongation of the bond. The host atoms in the vicinity of the chlorine molecule, which are not directly hit by the chlorine atoms, will start to react directly after the excitation of the molecule. This is connected to the change in spatial part of the electronic wavefunction and to the forces which evolve due to the motion of the chlorine atoms. The impulsive excitation of oscillations of the lattice atoms, as predicted by the DECP mechanism, will be discussed in section 6.7.1.4. In the C-state excitation, the effect due to the motion of the chlorine atoms is dominant, but for excitations with less energy, like B-state excitation, the displacive excitation of lattice atoms will be more apparent. Here the primary effect is just the movement of the chlorine in the available space given by the ground state geometry.

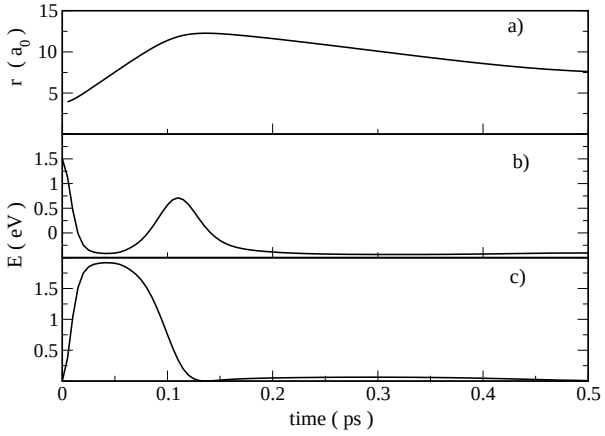

Figure 6.9: *a) Cl-Cl distance, b) potential energy (Cl_2), c) kinetic energy Cl_2*

Fig. 6.9 shows the distance of the chlorine atoms and the kinetic and potential

energy of each chlorine atom versus time. The chlorine starts to dissociate until it comes to the vicinity of the collision atom, after ≈ 100 fs. Here, on elastic impact, it looses most of its kinetic energy by momentum transfer. The chlorine atoms have only very small amount of kinetic energy left and thus the internuclear distance slowly starts to shorten again. Panel b) shows the potential energy for Cl_2 during the dynamics. The part of the C-state in the Franck-Condon-region is strongly repulsive and after 35 femtoseconds the minimum of the C-state potential is reached. Comparing all three panels there can be seen that then the molecule comes to the vicinity of the collision atom and therefore the potential is rising again. At the same time the momentum is transferred to this atom and after 135 femtoseconds the largest Cl-Cl distance is reached. Now the potential energy is decreasing again, due to the movement of the collision partner in z-direction away from the Cl atoms and due to the shortening of the Cl-Cl bond.

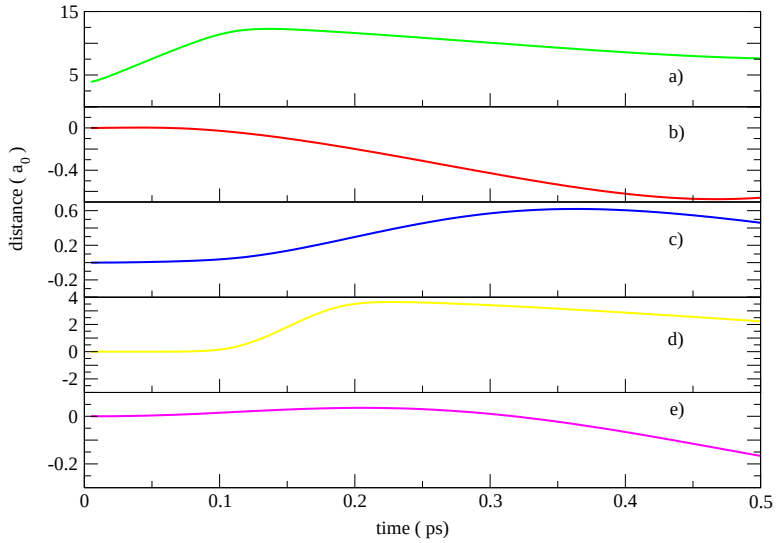

Figure 6.10: *Displacements of lattice atoms after excitation of Cl_2 to the C-state. a) Cl-Cl distance, b) belt atoms, c) window atoms, d) collision atoms, e) phonon atoms*

The behaviour of the surrounding atoms can be seen from Fig. 6.10, showing the distance to their initial positions and for comparison the Cl-Cl distance in

panel a). After photoexcitation and following elongation of the Cl-Cl bond, the belt atoms, which have been pushed outwards due to the chlorine molecule, will start to move inwards in the free space left by the dissociating chlorine atoms. This movement will close the belt and may hinder recombination in this state. The window atoms will start to move after ≈100 fs, due to the repulsion of the chlorine atoms, which have then reached the center of these windows. Shortly after the initialization of this motion the chlorine atoms will reach the vicinity of the collision atoms. The kinetic energy is transferred to these atoms and therefore they start to move in $\{110\}$ direction. In this simulation the displacement of the phonon atoms is only very small, compared to the other groups of atoms, the largest displacement is barely larger than that of the thermic oscillations in the lattice, which would lead to an average amplitude of 0.1 a_0, as determined by simulations performed in the ground state. A pronounced effect of this group of atoms in the C-state dynamics can not be seen, the excitation of the chlorine atom may result in a displacement of the phonon atoms, as discussed in section 1.4.2, but in fact the simulation time is too short and the kinetic energy of the chlorine atoms is too high for these atoms to adjust to the changed geometry of the system. This means, the wavefunction of the chromophore will expand, but the new equilibrium geometry with respect to the phonon atoms is not mainly influenced by this displacive excitation, but instead due to the change in geometry resulting from the space left by the dissociating Cl-atoms. From visualizations the behaviour of the cage and guest atoms can be seen more clearly. Fig. 6.11 shows some snapshots of these vizualizations with view from above, like shown in Fig. 6.3, including the spatial distribution of the wavefunction in the C-state. After collision with the cage, the wavefunction may undergo a state transition to the $^3\Pi$ state. The spatial distribution in those states is the same, the only difference being in the spin character. This spin-flip is not included in the classical dynamics performed here (see discussion, section 6.8).

This simulation shows, that the dominant interaction between chromophore and lattice results from the collision atoms. The behaviour of the different groups of atoms is reflected by the trajectory described in combination with the two-dimensional potential surfaces: excitation of the chromophore will lead to dissociation, until stopped by the repulsive wall due to the collision atoms. Here, the trajectory will be reflected and the Ar-Ar distance will elongate, while the Cl-Cl bondlength is decreasing slowly. The contribution of the other groups of atoms is less important, at least in the first 500 fs.

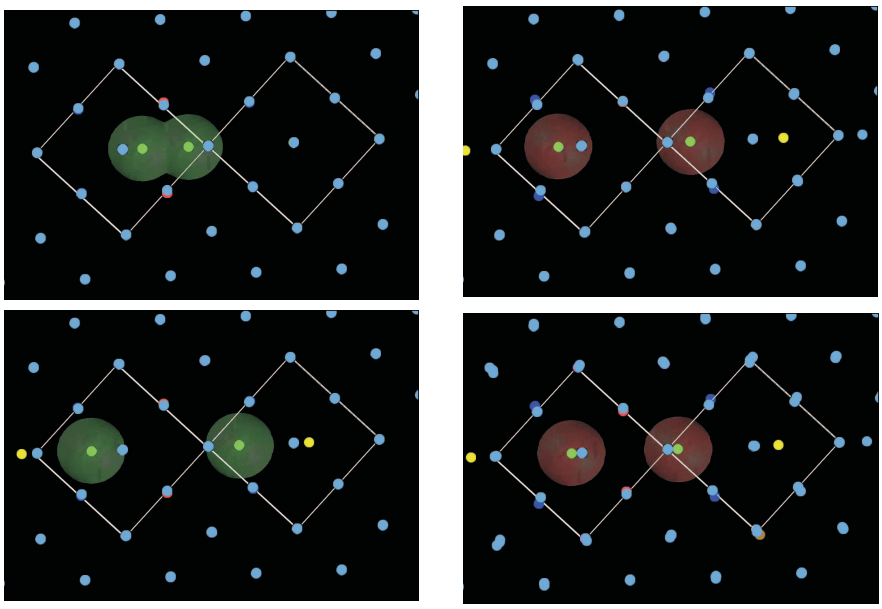

Figure 6.11: *Snapshots of the dynamics after excitation of Cl_2 to the C-state, from top left to bottom right at 0 fs, 120 fs, 240 fs, 400 fs. The solid lines depict the unit cell, see Fig. 6.2, the red and green clouds the distribution of the wave function. The change in color corresponds to a possible change in spin character from singlet (green) to triplet (red)*

6.6.1 Energy Distribution in the Lattice

6.6.1.1 Shock Wave

Due to the very similar mass ratio of chlorine and argon (m_{Cl}/m_{Ar} = 1.07), the kinetic energy of the chlorine atoms is mostly transferred to the collision atoms on impact. After the collision, the affected argon atoms start to move and hit the next argon atom in $\{110\}$ direction, see section 1.4, Fig. 1.6. In this way the kinetic energy is transported through the lattice. Displacements of the argon atoms belonging to this 'chain' can be seen from Fig. 6.12. After 566 fs the last atom leaves the boundary box and reenters on the other side with inverse direction of momentum, leading to incorrect results for longer propagation times.

Like mentioned before in section 1.4, this behaviour can be directly compared to the shock waves calculated for iodine in krypton, by changing the mass ratio between guest and host atoms to 1.0, as performed by Martens [43], compare Fig. 1.7 and the upper panel of Fig. 6.12. In agreement to the calculations of Martens,

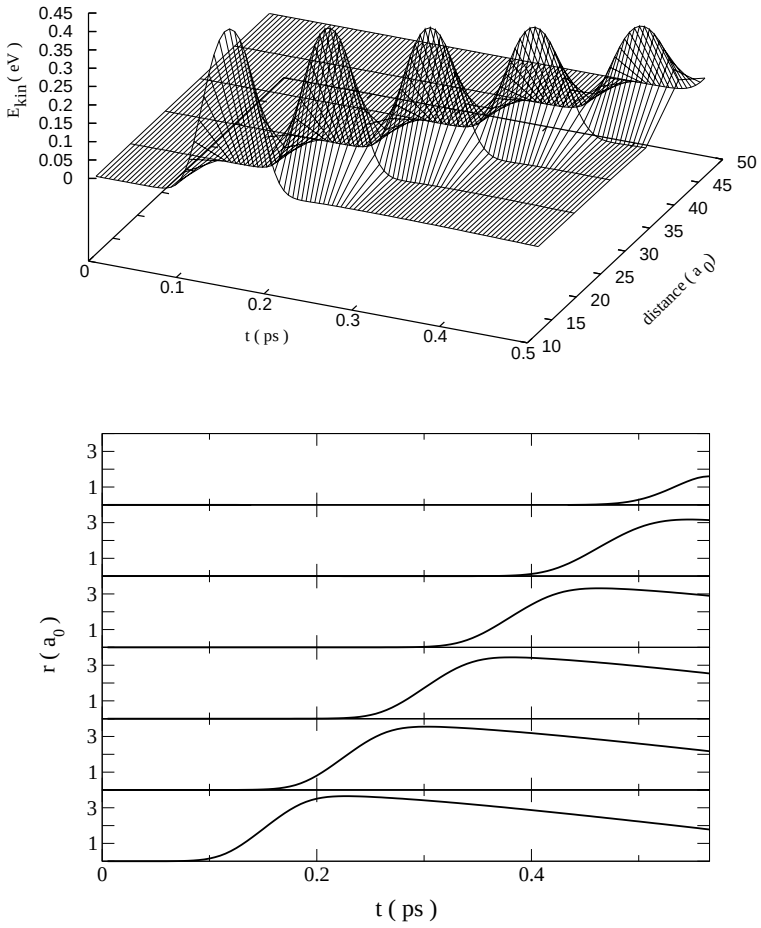

Figure 6.12: *Shock wave initialized by photoexcitation of Cl_2 to the C-state. Kinetic energy distribution along $\{110\}$ direction (upper panel). Displacements for the argon atoms constituting the shock wave (lower panel)*

shown in panel a) of Fig. 1.7, one shock wave can be seen travelling through the lattice, as can be expected by the mass ratio of chlorine and argon. The collisions are elastic, so the distance, which is covered by this shock wave, exceeds the size of the boundary box used in this simulation.

One feature discussed by Martens and also Gabriel, who investigated shock waves in pure Ar crystal [37], has to be emphasized: since this channel of energy transfer is most effective, the usage of periodic boundary conditions could be problematic, especially when the energy transfer is optimal like in Cl_2 in argon. When the last atom in $\{110\}$ direction reaches the end of the box, it will continue

and reappear on the other side of the box. This is of course not the case in reality, and from this time on the calculations are not valid anymore. For a small lattice with only three unit cells in each direction, the calculations were distorted after already 200 femtoseconds and so an appropriate box size has to be chosen, which is also connected to the excess energy given to the molecule. For all of the calculation performed here a lattice was constructed containing six unit cells in each direction for accessing reasonable propagation times of 566 femtoseconds.
The shock wave will be the major contribution to the total energy of the system. Fig. 6.13 shows the kinetic energy of the involved argon atoms (upper panel) and compared to this in the lower panel the total potential energy (solid line) and the potential energy of the chlorine as dashed line. The oscillations in the total potential energy are due to the progression of the shock wave through the lattice.
The shape of the kinetic energy shown in Fig. 6.13 indicates the softness of the

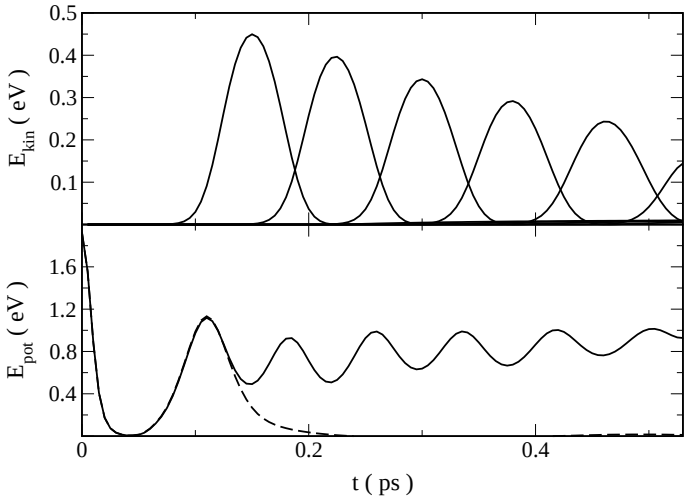

Figure 6.13: *Contribution of the shock wave to the total energy of the system. Upper panel: kinetic energy of the argon atoms along* $\{110\}$*. Lower panel: total potential energy of the system (solid line) compared to contribution from the guest molecule (dashed line)*

Cl-Ar potential. In contrast to a hard potential, the kinetic energy is not given instantly from one atom to the next one in the chain. The oscillations in the total potential energy of the system thus resemble the behaviour of the kinetic energy of the argon atoms as shown in the upper panel. The potential energy of the system

will rise until the kinetic energy is given to the next atom, which can be seen from the intersections of the kinetic energy in the upper panel. The next atom in the 'chain' will then start to move, and thus the potential energy is decreasing again until it rises again due to the next argon atom. In addition, the kinetic energy of the atoms constituting the shock wave is decreasing, which indicates some energy dissipation off this main axis and will be discussed in the next section.

6.6.1.2 Energy Distribution in Different Layers

Not only the energy distribution in the direction of the molecular axis was investigated, but the energy distribution in different layers. Different groups of atoms, characterized in Fig. 6.2 will react to the photodissociation dynamics of the chlorine molecule. The left column of Fig. 6.14 shows contour plots of the displacements of lattice atoms in the layer above the chlorine molecule. This layer contains belt and window atoms. Closest in distance to the center of mass of the chlorine molecule are the belt atoms. They will only gain a very small amount of energy in the first round trip. Their displacement starts because of the lack of repulsive forces, due to dissociation of the chlorine molecule and their movement to the free space left by the Cl-fragments. When the chlorine returns to the inner turning point of the potential, according to the smallest Cl-Cl bond length, the now slightly closed belt will be opened by the chlorine again. The movement of the belt atoms is primary perpendicular to the molecular axis, compare to the snapshots shown in Fig. 6.11. The displacements in x and y direction are small, compared to displacements above/below the layer.
The largest displacement can be assigned to the window atoms, which will be pushed outwards by the chlorine atoms, which pass through the center of these windows at the bond elongation. After collision of the guest molecule with the cage, the next collision atoms start to move and pass through the same kind of windows. Fig. 6.15 shows the displacement of the atoms containing the first and second layer at snapshots taken at 400 and 500 fs. On the left panel, the first layer above/below the chlorine layer, shows the opening of the next windows, at 500 fs the atoms constituting the shock wave nearly reaches the end of the box and so the windows nearly to the end of the box have been opened. For the windows atoms the displacement will be mainly in the direction perpendicular to the molecular axis, above and below their initial layer, but from Fig. 6.14 and Fig. 6.11 it can be seen, that they will be displaced also in x and y direction as defined in Fig. 6.14.

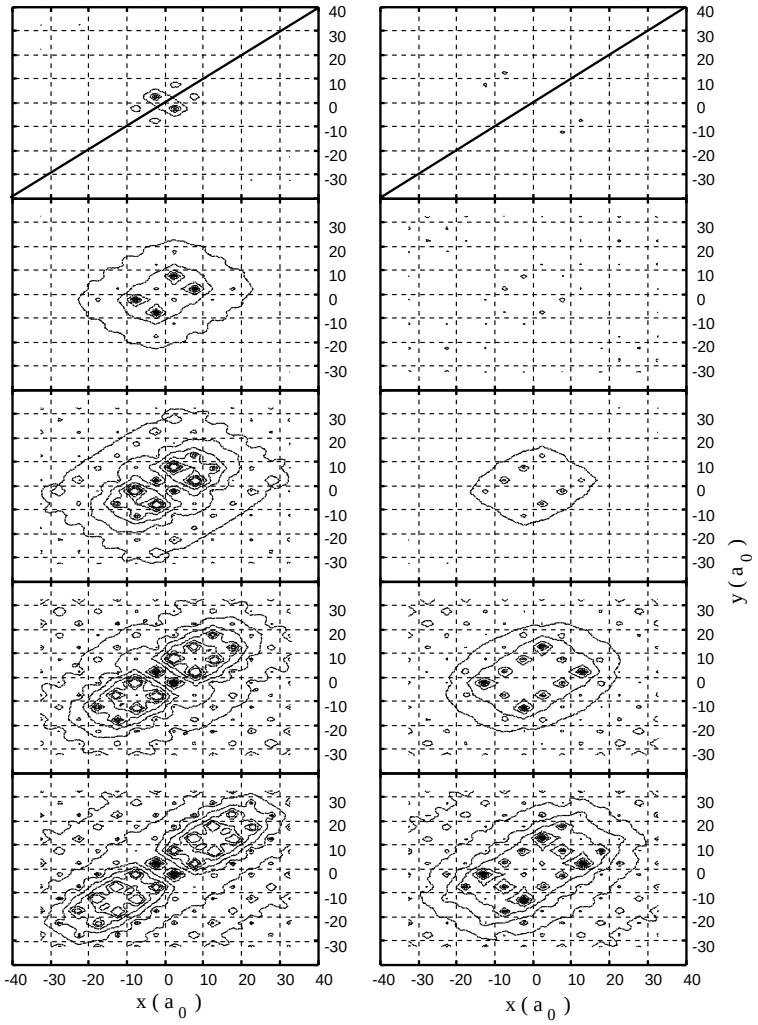

Figure 6.14: *Displacement of atoms from their initial positions in layers above/below the one containing the chlorine. Left column: one layer above chlorine layer, right column: two layers above chlorine layer. The rows are showing snapshots from top to bottom at 100, 200, 300, 400 and 500 fs. The solid line in the upper panels indicates* $\{110\}$ *direction. The contour lines show the displacements perpendicular to this axis, x and y are the coordinates in the respective layer.*

The second layer will also be influenced by the dynamics of the chlorine molecule. When belt, window or the other atoms in the first layer are displaced, they will affect the atoms in the next layer and start oscillations there. Fig. 6.14 shows that the propagation is now affecting even more atoms in this layer. Since

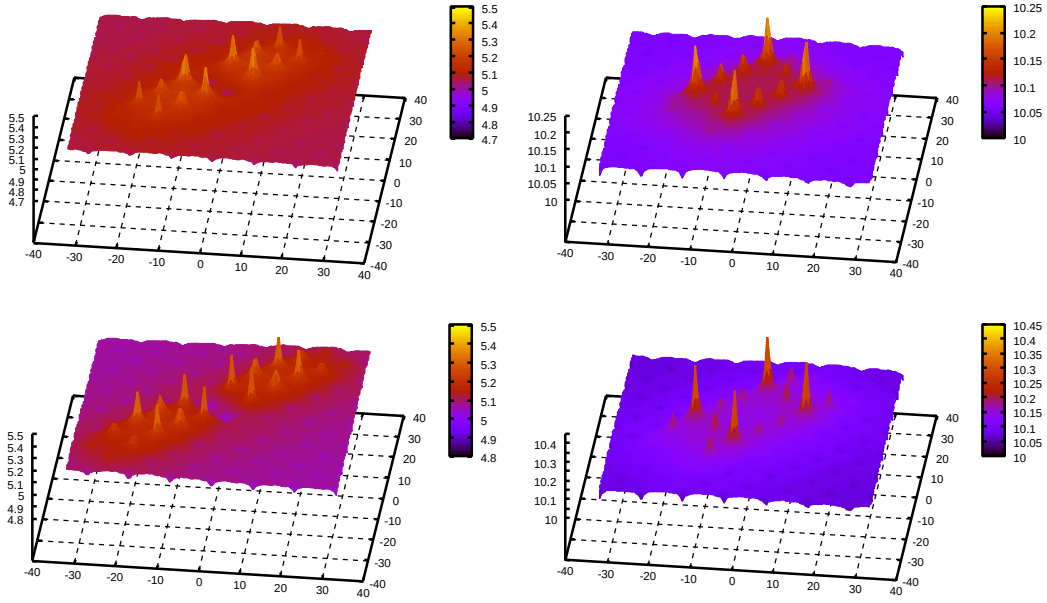

Figure 6.15: *Displacement of atoms in layers above/below the one containing the chlorine. Left column: one layer above chlorine layer, right column: two layers above chlorine layer. The rows are showing snapshots of displacement in z-direction at 400 fs (top) and 500 fs (bottom). Compare Fig. 6.12*

the Cl-Cl axis is on the diagonal, we see even more distribution of energy in the direction perpendicular to it. The mechanism for this energy distribution is the opening of the belt and window atoms, which will start oscillations in the next layer, like for example the atoms above the window atoms shown in Fig. 6.2.
Summarizing, the energy distribution, shown by the displacements or oscillations initialized in layers above and below the layer containing the chlorine molecule is short ranged, the influence of the guest dynamics on atoms in the forth layer are already negligible. The distribution will spread in directions off the main axis. Oscillations initialized in the layers above or below the chlorine molecule can affect the dissociation dynamics of the chromophore seriously, for example by back transfer of momentum to the chlorine fragments. The problems arising due to the shock wave and the boundary conditions of the system can be avoided by generation of a different box size, with expansion mainly in the direction of the molecular axis. Still four layers above and below, respectively, should be included to reflect the correct behaviour of the system.

6.7 B-state Excitation

The excitation to the B-state of Cl_2 in Argon was experimentally investigated by the groups of Bondybey [20] and Schwentner [40]. As shown in chapter 3, Fig. 3.3, the excitation spectrum of Cl_2 in Ar has distinct contribution from the phonon side bands for the higher vibrational levels of the B-state. In addition, the pump probe spectrum Fig. 3.4 shows a similar behaviour for C- or B-state excitation, presumably due to a nonadiabatic transition from the C-state to the energetically lower B-state. Oscillation periods, determined from these pump probe spectra, see also Fig. 3.5, can be compared directly to the simulations. Also experimental measurements for the rate constants of the vibrational relaxation exist, see Fig. 1.14.
Stimulated by these experimental results, the dynamics of the system after excitation to the B-state was performed. Franck-Condon excitation to the B-state of

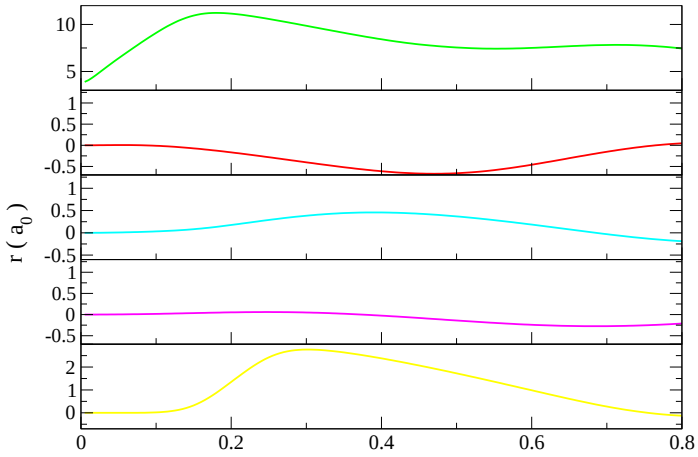

Figure 6.16: *Displacements of lattice atoms after excitation of Cl_2 to the C-state. a) Cl-Cl distance, b) belt atoms, c) window atoms, d) collision atoms and e) phonon atoms.*

chlorine in argon is very similar to the C-state excitation, compare Fig. 6.16 and 6.10. Again the belt atoms move inwards, the window atoms are pushed outwards and the momentum is transferred to the collision atoms. There are no significant differences to the C-state excitation, especially belt and phonon atoms show only

small deviations. The most significant difference is due to the smaller excess kinetic energy of the chlorine atoms. Movement of the collision atoms starts 40 fs later with less momentum transferred from chlorine to argon.
Again, a shock wave is initialized and the calculations will be correct until 820 fs, when the last atom leaves the boundary box. The kinetic energy of this last argon atom is much lower than in the C-state excitation, like shown in Fig. 6.17, and the inversion of the direction of the shock wave is negligible, unlike in the case for the excitation to the C-state compare to Fig. 6.12. The excess energy of the last atom in the chain is dissipating in the outer regions of the boundary box and will not influence the dynamics of the chromophore. This gives the opportunity of calculating long time dynamics and a comparison of the lattice dynamics with respect to the long living phonon modes.

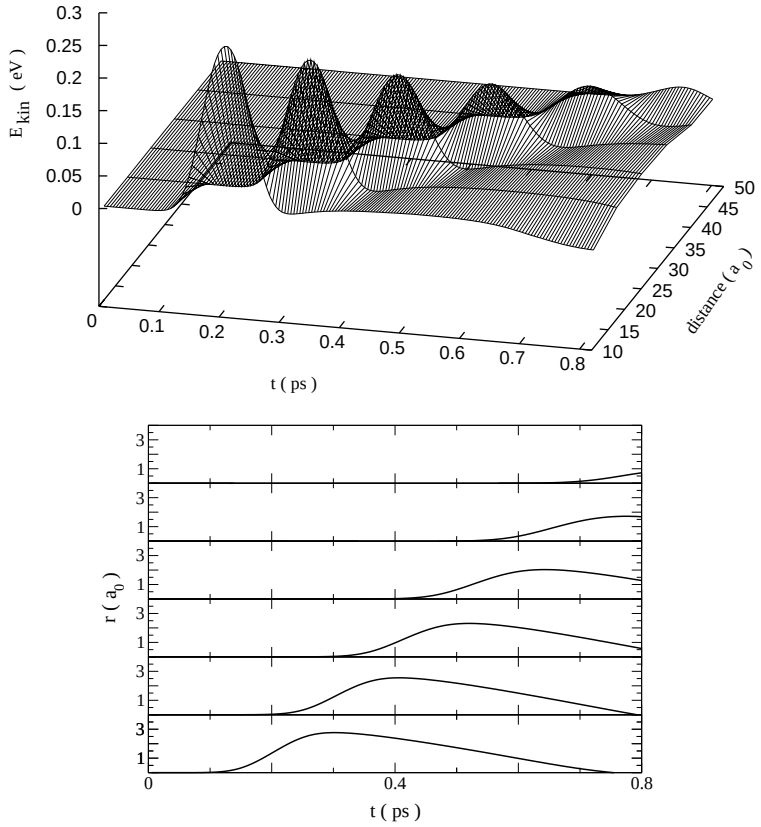

Figure 6.17: *Shock wave initialized at photoexcitation of Cl_2 to the B-state. Kinetic energy distribution of the argon atoms in $\{110\}$ direction (upper panel), displacement of these argon atoms (lower panel)*

6.7.1 Energy Distribution with Different Initial Energies

To monitor the vibrational relaxation in the B-state, model calculations were performed. From pump-probe experiments data is available to the energy relaxation in the B-state, see Fig. 1.14. The pump-probe scheme, as discussed in section 1.5.1.1 monitors the energy loss after pumping with different initial energies and this will provide the relaxation rate.

$$k_{rel} = \frac{dE}{dt} = \frac{E_i - E_j}{t_i - t_j} \tag{6.3}$$

As shown in Figure 1.13 the difference in energy per difference in time can be measured and from plotting this against the excess energy the relaxation rate can be determined. After Franck-Condon excitation from the ground to the B state, the chlorine starts to dissociate and hits the cage, transferring momentum to the collision atoms and relaxing to the bound part of the potential.
To simulate this energy loss at the collision, the total energy of the chlorine $E_{pot} + E_{kin}$ is measured before and after the collision. This is performed for different excitation energies, respectively different Cl-Cl distances.

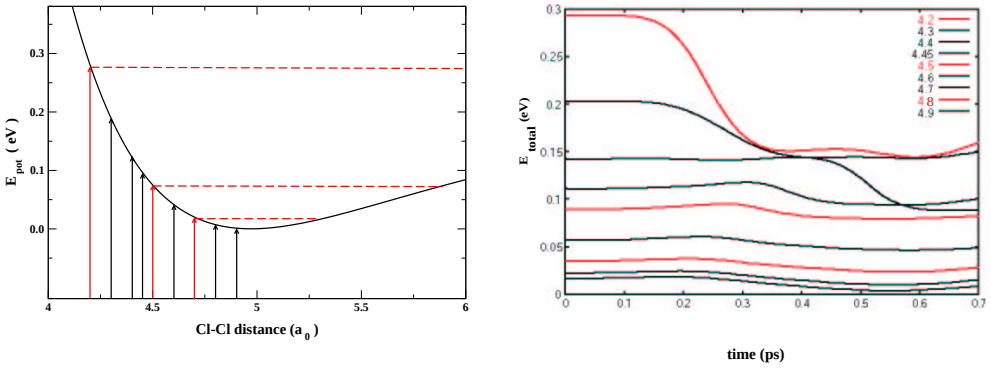

Figure 6.18: *Representative overview of r_{Cl-Cl} taken for simulation of the vibrational relaxation (left) and corresponding change in total energy of Cl_2 (right).*

As a zero order approximation the relaxed ground state geometry is taken and the Cl-Cl distance is prolongated artificially. The vibrational states $v' <=$ 10 can be achieved experimentally from excitation X $\rightarrow$ B, to excite at larger Cl-Cl distances a pre-exitation would be required. This pre-exitation would then result also in an excitation of the lattice atoms, restricting the comparison to these

results. The simulations are all starting from the relaxed ground state geometry, where only the Cl-Cl distance is shifted artificially. The calculations were carried out assuming 0 K as temperature. An overview of the different distances can be seen from Fig. 6.18. For better perception the minimum of the B-state is set energetically as zero.

The total energy of chlorine, shown in panel (b) of Fig. 6.18 and in Fig. 6.19 shows no clear trend. Two tendencies can be extracted: for the initial energies above the dissociation limit (small Cl-Cl distances at excitation, see left panel of Fig. 6.19) the energy loss is large and with enlarging the distances up to 4.4 a_0 there is a trend of the energy loss getting smaller at later times. Then a second trend sets in, the energy loss is only a fraction of the energy loss of the high energy excitations and happens earlier (right panel of Fig. 6.19). Two different mechanisms of energy dissipation can be assumed and a study of the underlying lattice dynamics will give insight in these different channels for energy dissipation. These two trends can also be extracted from the behaviour of the relaxation rate as shown in Fig. 1.14. Above the dissociation limit the slope of the k_{rel} is

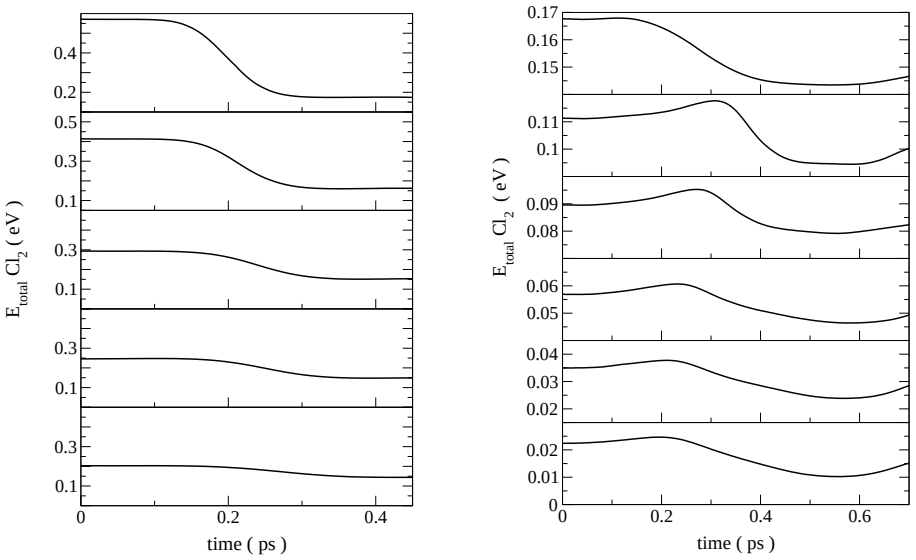

Figure 6.19: *Change in total energy of Cl_2 for different initial bond length: left: excitation above the dissociation limit at r_{Cl-Cl} = 4.0, 4.1, 4.2, 4.25, 4.3 a_0 (top to bottom), right: excitation above the dissociation limit (top) and below at r_{Cl-Cl} = 4.35, 4.5, 4.6, 4.7, 4.75, 4.8 a_0.*

different from excitation into the potential well, since in the latter case the interaction with the lattice is much smaller.
It is evident, that in the case of higher excitation energies the amount of energy loss upon collision can be determined. In the other cases, the determination of this quantity is more difficult, because of the rise of the total energy in the time prior to the energy loss. The first step is to resolve the mechanisms for energy distribution, and three different cases will be discussed, with excitation above the dissociation limit, to the bound part of the potential but near the dissociation limit and near the potential minimum.

6.7.1.1 Excitation Above the Dissociation Limit

For excitations above the potential well, an internuclear distance of Cl_2 of 4.2 a_0 is taken as example. The corresponding energy is lower than in the case of Franck-Condon excitation and thus the initialized shock wave will have less energy. This can be seen in Fig. 6.20, where even after 2 ps the energy is already distributed in the lattice.

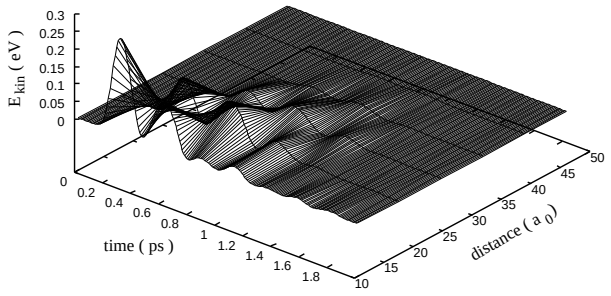

Figure 6.20: *Kinetic energy of argon atoms constituting the shock wave. Simulations are valid for a time $>$ 2 ps since the last atom will not get sufficient energy to leave the boundary box*

The last argon atom in the chain will not get sufficient energy to leave the simulation box and this gives the opportunity to calculate the system's behaviour on a longer time scale. The simulation shows principally the same behaviour like in the case of Franck-Condon excitation discussed in the previous section, see Fig. 6.21.

The upper panel of Fig. 6.21 shows the displacements of the important groups of atoms, but now on a longer time scale. The fundamental behaviour stays the

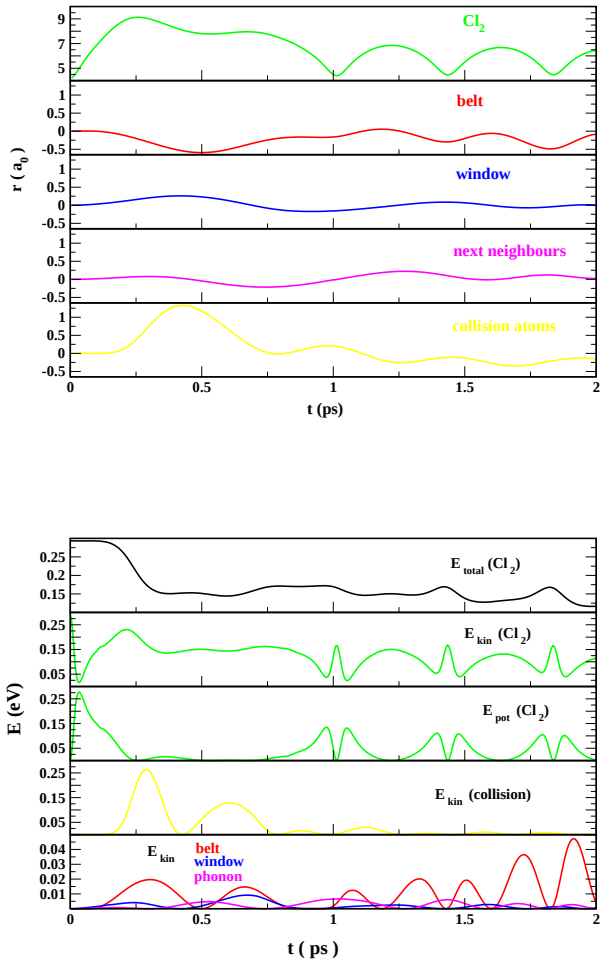

Figure 6.21: *Top: Displacements of the important group of atoms with respect to their initial positions after excitation at* r_{Cl-Cl} *= 4.2* a_0*. Bottom: corresponding energies compared to* E_{total} *(*Cl_2*).*

same as in the case of Franck-Condon excitation. For t $<$ 0.866 ps it can be directly compared to Fig. 6.16, showing the displacements after Franck-Condon excitation. Now on a longer time scale, all of the atoms start oscillating and after 1 ps their behaviour becomes more regular. Most interesting in this respect is the behaviour of the Cl-Cl distance: while first the displacement is large , after 1 ps a shorter internuclear distance is reached again and after that the molecule starts oscillating with a lower frequency and a smaller elongation of the bond. This indicates that the molecule has now relaxed into the bound part of the potential

and the largest bond length now accessible is restricted by the chlorine potential. This is reflected in the lower panel, showing the energies of these groups of atoms. In the same way the potential energy of the halogen is decreasing, the atoms are accelerated. The potential energy is increasing again when it comes into the vicinity of the cage wall and there the momentum is transferred to the collision atoms. The kinetic energy of belt, window and phonon atoms is approximately ten times smaller, since they just react to the modified potential due to excitation and dynamics of the guest molecule. The oscillation of the chlorine in the potential well shows different properties. First, there will be no second momentum transfer from the chromophore to the collision atoms. Second, the kinetic energy of the belt atoms is increasing at times, where the Cl-Cl distance is shortened and we see from the panels with the chlorine kinetic and potential energy, that the inner turning point is reached. This indicates a different mechanism for the energy loss for times > 1 ps, but this is not reflected in the trend of the total energy of the guest molecule as shown in Fig. 6.18, which is only taking into account the first loss of energy. The energy loss for Cl_2 below the dissociation limit will be discussed in the next section.
The phonon atoms as next neighbours in the same layer as the chlorine molecule seem to be displaced slightly after the excitation and start to oscillate. Their kinetic energy and their shifting is much less pronounced than for the other groups of important atoms. Still their behaviour is interesting, since it could be connected to the long living phonon mode observed by Apkarian and Schwentner [60, 66]. They are not so much involved in the dynamics at higher excitation energies and thus their contribution will be discussed in context with the excitation near the potential minimum and the role of the wavefunction, section 6.7.1.4.
The trajectories at 0 K well represent the behaviour of the system. For comparisons an ensemble of 23 trajectories at 4 K with different initial conditions, due to a Boltzmann distribution of the atoms was simulated. Weighting of these trajectories with respect to the energy of the system showed no fundamental deviation from the behaviour of the system which can be seen in Fig. 6.21.

After analyzing the data of the other excitations above the dissociation limit of the B-state we are now able to explain the first trend in the total energy of the Cl_2 as shown in Fig. 6.18. The dominant contribution to this channel for energy relaxation is momentum transfer to the collision atoms. The energy loss is expected to be large, due to the similar masses of chlorine and argon. In addition,

the time of the energy loss can be well connected to this collision event. Elongating the bond, as reflected in Fig. 6.18, will just lower the initial energy of the chromophore. It will gain less kinetic energy and thus will take longer time until it reaches the outer turning point, when momentum is transferred to the collision atoms. From the potentials shown in Fig. 6.4 the outer turning point of all these excitations above the dissociation limit is due to the repulsion from the collision atoms, which is very similar for all of these excitations. The amount of energy transferred to the lattice at the outer turning point is getting smaller, but still in relation to the initial amount of energy. The proportion of momentum transfer is nearly the same for all these different initial energies.
Another trend setting in for excitation with lower energies can also be seen from Fig. 6.18: while in the case of 4.2 a_0 the total energy of Cl_2 after excitation stayed nearly constant until the collision event, there can be seen a small increase for excitations at longer bond length/lower initial energy. Again this is a trend which is much more pronounced for the excitations below the dissociation limit and will be discussed in the next section. Here it should only be emphasized that even for energies above the dissociation limit more interactions with the lattice atoms have to be taken into account, which will influence the total energy of the chromophore. The determination of the energy loss becomes more difficult for trajectories with lower initial energy will become evident in the next section.

6.7.1.2 Excitation below dissociation limit

The second trend already sets in with the excitation at 4.4 a_0. Now the energy loss takes a longer time, but at the same time starts earlier and additionally the amount of energy lost is only a fraction of that from excitation above the dissociation limit. First the behaviour of the chromophore and of the important groups of rare gas atoms is discussed, which will lead to some conclusions with respect to the mechanism of guest-host interaction and the trend observed in the total energy of the chromophore.

The first difference, which is obvious for excitations below the dissociation limit is the increase of the total energy before the energy loss, see Fig. 6.19. From an ensemble of 29 trajectories it became evident, that this is no artefact, but instead is seen also after determining the mean value of the weighted trajectories. Comparing to the investigations performed in the group of Apkarian for iodine

in krypton [60] and the interaction model of section 1.4.2, one explanation for this increase could be that energy is transferred from the lattice to the chlorine molecule. The whole system is promoted to an excited state and the lattice atoms are not at their equilibrium distance anymore. The energy stored in the environment will lead to displacements of the host atoms and by this changing the potential energy of the guest molecule. This effect, related to the DECP mechanism mentioned in section 1.4 is different from energy dissipation to the lattice by momentum transfer in direct collisions. The same increase of energy can be seen at later times, especially when the fragments come into the vicinity of the closing windows and will be accelerated. The chlorine has much less kinetic energy here and is due to the reduced velocity more sensible to effects from the matrix. This could explain why this energy increase is not evident in the higher excitation trajectories. Since this effect should be more important for even lower energies, it will be discussed in the case of excitation down in the potential well.

For trajectories starting near the dissociation limit the distance Cl-Cl = 4.5 a_0 is taken as example. Here the second trend has already set in, enlarging the initial bond length will lead to an earlier energy loss, which will get less pronounced. When comparing the same amounts of energies and distances as in the previous case, one finds some significant differences. Again, Fig. 6.22 shows a representative trajectory from an ensemble of 29 trajectories, weighted with respect to the total energy of the system.

The behaviour of the chlorine shows immediately an oscillation with a period of 300 fs, the outer turning point is reached after approx. 180 fs. In contrast to the previous case with excitation above the dissociation limit, now the collision atoms are not pushed outwards by the chlorine atoms, but quite oppositely follow the halogen atoms on their way back. This movement starts when the Cl fragments come near to the collision atoms and continues even at the second time the chlorine reaches the outer turning point. The increase of kinetic energy of the collision atoms is much smaller than in the case discussed before. From this it becomes evident, that no momentum was transferred in a direct collision. The bond elongation of the chlorine is thus not restricted by the cage wall, but instead by the intramolecular potential. No shock wave will be created and so a different mechanism of energy exchange with the environment has to be applied.
This inward motion of the collision atoms, which reflects the volume conversa-

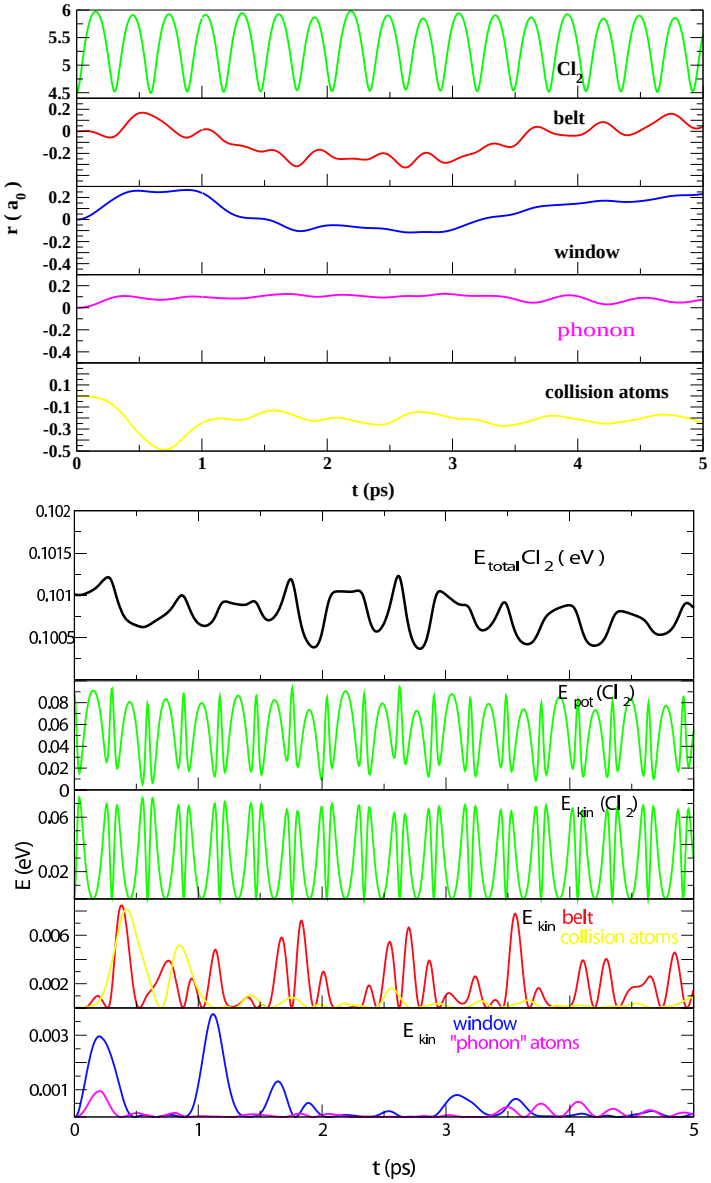

Figure 6.22: *Top: Displacements of the important group of atoms with respect to their initial positions after excitation at* r_{Cl-Cl} *= 4.5* a_0*. Bottom: corresponding energies compared to* E_{total} *(*Cl_2*).*

tion and could be triggered by the chlorine-argon attraction, is responsible for another effect: First the window atoms will be pushed outwards, due to the bond elongation of the chlorine atoms like in the previous case, but their displacement is restricted by the interaction with the atoms of the next layer. After reaching their largest displacement, they start closing again. At the time they reach their

initial positions, the collision atoms inhabit now the former free space of the window's center and restrict the further movement of these atoms. From Fig. 6.22 it can be seen that at this point nearly all of the kinetic energy of the window atoms is lost and they start moving again when the collision atoms are leaving the occupied space in the center of the windows.
Comparing the oscillation of the chlorine and the behaviour of the lattice atoms, the displacements of the environment are now much less influenced by the chromophore dynamics. Still from Fig. 6.18 a small energy loss in the total energy of the chlorine can be seen. This can not be attributed to the collision or window atoms, but instead energy decrease happens when the molecule reaches the *inner* turning point of the potential. At the same time the belt atoms, which moved into the vacancy left by the chlorine atoms, change their direction and open again. The most significant rise in the kinetic energy from these groups of lattice atoms can be attributed to the belt atoms, see Fig. 6.22. So at excitations high into the potential well the dominant contribution to the guest-host interaction comes from interaction with the belt atoms at the inner turning point of the Cl_2 potential.

It is clear that here another channel for energy relaxation in the lattice has to be applied. Now we can discuss the trend in the total energy of the chlorine, Fig. 6.18. The first difference to the excitation above the dissociation limit is the shallow increase in the first 300 femtoseconds. This was not evident from the trajectory with higher energy and initial bond length of 4.2 a_0 and there is no eye-catching explanation for this effect. One possible reason for this increase could be the displacement of the host atoms from their equilibrium configuration due to impulsive excitation of the chlorine to an excited state like in the DECP mechanism, see section 1.4.2. This excitation will promote the whole system to a non-equilibrium state. The host atoms will experience a force towards their new equilibrium positions and during the related motion the potential of the whole system will be affected. The amount of energy exchanged is very small and the appearance of this increase only at lower excitation energies is supposedly due to the smaller velocity of the chlorine atoms. Rearrangements of the lattice atoms and the resulting change in the total energy of the chromophore during the first bond stretching should be more pronounced if the system has enough time to adapt to the new situation.

The overall smaller loss of energy can be explained with the different mechanism of energy transfer to the environment. The efficiency of energy transfer to the lattice is optimal in the case of direct collisions with the lattice atoms, but reduced by the mechanism applied here. The long time behaviour of the total energy of Cl_2 can be seen from Fig. 6.23. At times, where the total energy of Cl_2 is decreasing, the molecule is at the inner turning point and the belt atoms are moving inwards. The belt atoms will gain some momentum and start to open again. The irregular structure of Fig. 6.23 is due to various rearrangements of the lattice atoms. Again the most notable contribution to the total energy is coupled to the displacement of the belt atoms, increasing the energy of the chromophore when moving inwards and this is accompanied by gaining momentum when they are pushed outwards again. So the first trend, the smaller amount of energy given

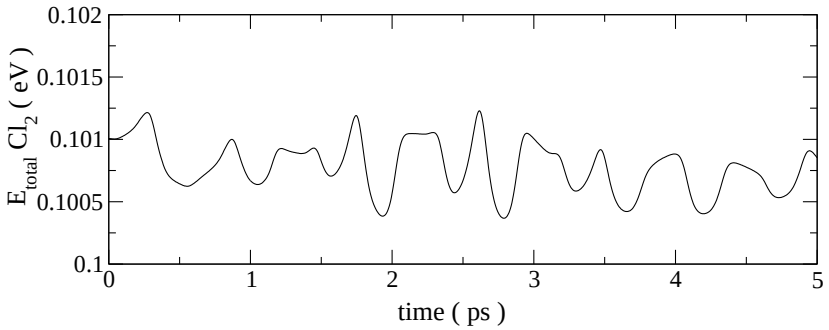

Figure 6.23: *Total energy of Cl_2 after excitation at r_{Cl-Cl} = 4.5 a_0.*

to the lattice, can be explained with a different mechanism of energy transfer. The second effect seen in Fig. 6.18 is the energy loss happening earlier with less initial energy/larger initial r_{Cl-Cl}. This effect is due to the anharmonicity of the potential. At the highest excitation *into* the potential well, the asymmetric shape of the potential would allow the largest stretching of the bond. The differences in kinetic energy get smaller and at the same time the obtainable bond length shortens.

6.7.1.3 Excitation Near the Potential Minimum

For the excitation near the potential minimum a Cl-Cl distance of 4.7 a_0 is chosen as example. The behaviour of the special groups of atoms stays nearly the same as in the previously discussed case, but by comparison with the excitation at 4.5 a_0,

the coupling between the belt atoms and the chromophore is even weaker. Again the belt atoms are responsible for the first energy loss, but all the energies and displacements are very small, most pronounced for the collision atoms, which will move inward again. The oscillation period of chlorine is around 200 fs. Displacements and energies are shown in Fig. 6.24.

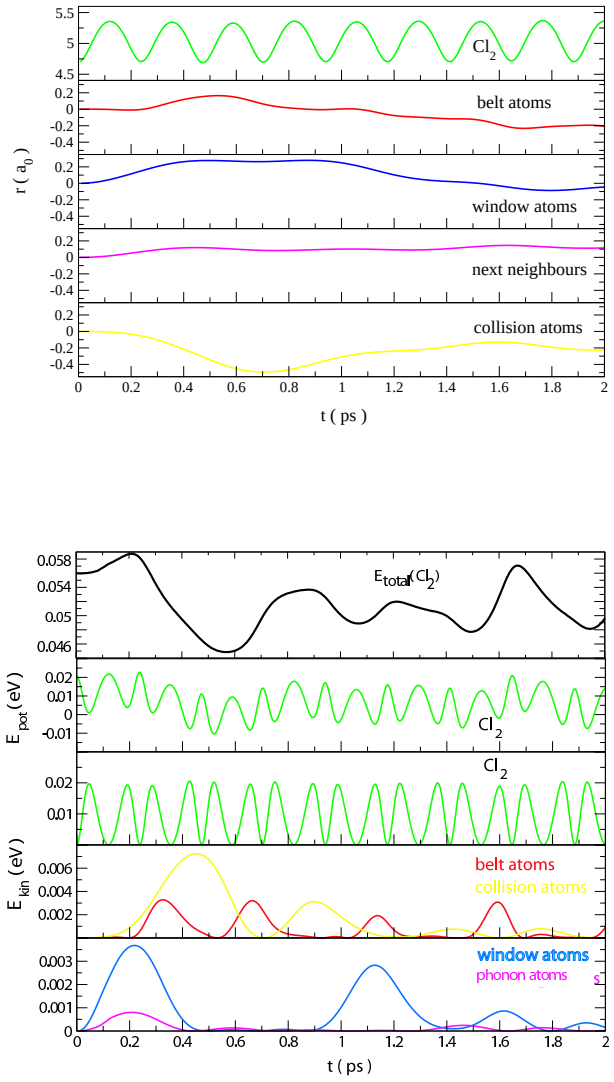

Figure 6.24: *Top: Displacements of the important group of atoms with respect to their initial positions after excitation at r_{Cl-Cl} = 4.7 a_0. Bottom: corresponding energies.*

The excitation near the potential minimum is still following the same trend as in the section before, but with less initial energy: The energy loss is in the range of that for excitation near the dissociation limit, but even smaller. Compared to this it occurs faster, after approx. 200 fs, due to the asymmetric shape of the potential as discussed above.
Again the rise of total energy of Cl_2 is evident and like in the previous case the energy is lost to some amount at the inner turning point. Here it can be seen that the belt atoms get even less kinetic energy, only half of the kinetic energy of the collision atoms. The influence of the guest dynamics on the behaviour of the system is less than in the case of excitation at 4.5 a_0, so the system is nearly decoupled. This corresponds to the observations of Bondybey [20], where a very weak coupling was found for vibrational levels near the minimum of the B-state potential as discussed in chapter 3. There is some decrease in the potential energy of the chlorine molecule, depending obviously on the behaviour of the belt atoms, but since all these energies are small the kinetic energy of the lattice atoms following a Boltzmann distribution at temperature > 0 K could cancel out even these effects. If the molecule is oscillating deeply in the well, a factor which appeared already in the previous sections will gain influence, namely the induced displacement of the argon atoms by electronic excitation of the chromophore, which will be discussed in the next section.

6.7.1.4 The Role of the Wavefunction

The relaxed geometries in the ground and in the B-state are shown in Fig. 6.25. The important features of the ground state were already described in section 6.2. The relaxed geometry of the B-state shows some small differences, due to the enlarged bond length of the chlorine molecule and the different spatial distribution of the wavefunction. The minimum in potential energy of the B-state has its minimum at r = 4.96 a_0. This means the chlorine atoms are near to the locations of the removed argon atoms. For the *window* atoms this means, compared to the ground state, not so much space and more repulsion from the chlorine. They will be pushed outwards. The *belt* atoms, on the other hand, have more space and a longer distance to the chlorine atoms, but they stay on their positions, this effect could be explained with the changed wavefunction's distribution in x- and y- direction. Their distance to the chromophore atoms is

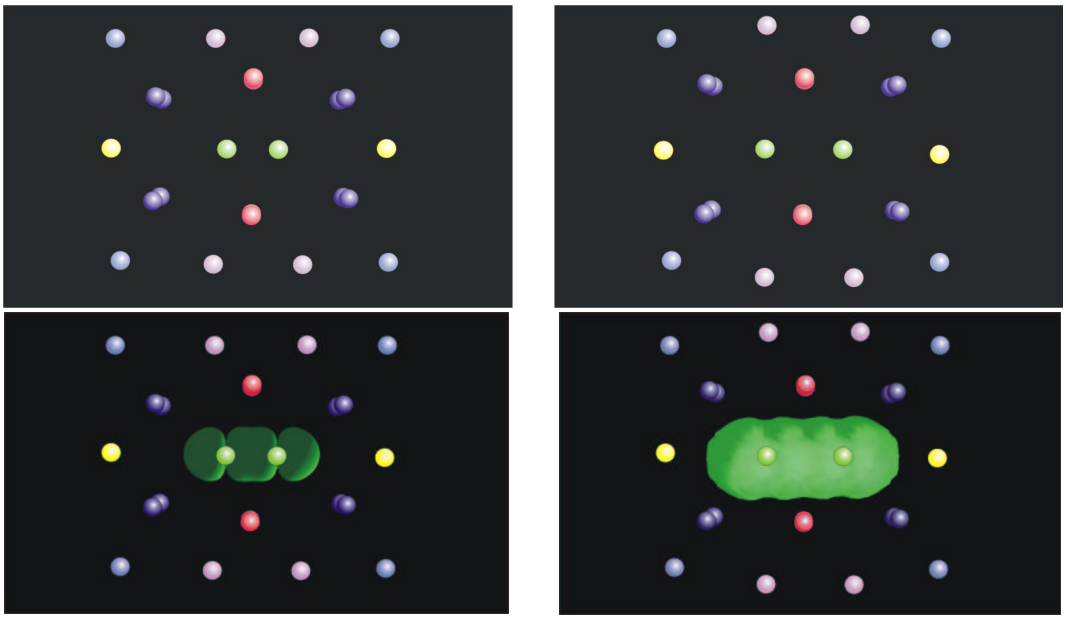

Figure 6.25: *Comparison between the relaxed geometries in ground (left) and B-state (right). The lower panel shows the distribution of the* $^1\Sigma$ *and* $^3\Pi$ *wavefunction, respectively.*

enlarged, thus it can be expected that they would take the position they would have in a regular argon lattice. On the other hand the space inhabited by the $^3\Pi$ wavefunction is larger than that of the ground state, which has main contribution along the molecular axis (the overlapping of the p_z-orbitals). The relaxation of these atoms due to the larger Cl-Ar distance is compensated by this repulsion, so the belt atoms will occupy the same locations as in the ground state.

The *collision* atoms show no significant adjustment to this new situation. This is interesting, because this means the movement towards the chlorine center of mass, observed in the last two simulations at 4.5 and 4.7 a_0 , should therefore be initiated by the Cl-Ar interaction at the largest r_{Cl-Cl}. Probably most interesting is the behaviour of the *phonon* atoms, which are pushed slightly outwards, also due to the wavefunction distribution. Since the collision, window and belt atoms will be directly involved in the dynamics, influence of the chromophore on the phonon atoms follows a different mechanism. The main reason of their displacement is the change in the wavefunction, so after excitation they react to the forces towards their new equilibrium positions, see Fig. 6.25, until finally they oscillate around these new coordinates. Of course this is not completely decoupled from

the movement of other atoms, but the initiation of this process could be identified by the DECP mechanism. The initialization of these oscillations could start a local mode of the lattice, but investigations including normal mode analysis of the lattice should be performed to validate this. Another argument for the involvement of these phonon atoms for the long-living oscillations (like for I_2 in Krypton or Br_2 in Argon) is that motions of the lattice, induced by direct collision with the chlorine or with motions coupled to the chlorine motion, should be damped rapidly. This is not the case if only local modes of the lattice are excited. Apkarian and coworkers claimed this mechanism for iodine in krypton, where they made the belt atoms responsible for this long living phonon modes, while Schwentner et al. proposed the next neighbours to be involved in these modes.
From the calculations performed here, there is much evidence that the next neighbours, or phonon atoms, as called here, are influenced by the excitation of the chlorine molecule to the B-state, and that their new equilibrium geometry is connected with the spatial change of the wavefunction, thus inducing their movement towards the new equilibrium positions. For connecting them to the long living phonon mode more investigations have to be performed.

6.7.1.5 Lattice Vibrations

For investigation of the long time behaviour of the system, simulations up to 10 ps were performed. While in the first 2-3 ps the system is adapting to the new situation, the atoms establish subsequently a more periodic behaviour. Fig. 6.26 shows the long time behaviour of the system with excitation above the dissociation limit, according to intramolecular Cl-Cl distances of 4.2 a_0 and 4.5 a_0, respectively.

For the excitation with higher initial energy, on the left panel, it can be seen that especially the oscillations of belt and collision atoms shows a more periodic behaviour for $t > 3$ ps. Cl_2 shows first a large elongation of the bond, then the maximum bond length becomes shorter for two oscillation periods with a maximum of 6.9 a_0, two with maximum 6.5 a_0 after a small increase it shortens again until it finally has its maximum at 5.9 a_0. After reaching this intramolecular distance, it does not shorten significantly, which means that now the guest-host dynamics are nearly uncoupled. For $t > 3$ ps the displacements of the atoms adapt to a large

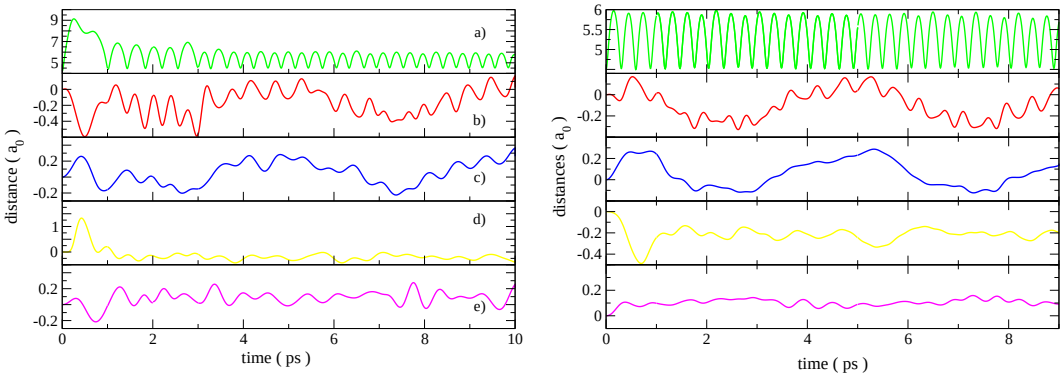

Figure 6.26: *Comparison of the long time dynamics for excitation above the dissociation limit at r_{Cl-Cl} = 4.2 a_0 (left) and below the dissociation limit at r_{Cl-Cl} = 4.5 a_0.*

oscillation period for especially window and belt atoms, showing an underlying smaller one. The same picture then is reflected in the right panel, showing the excitation at a Cl-Cl bond length of 4.5 a_0. As discussed in the previous sections, the collision atoms show the most significant difference, please note that the scaling is changed from the left to the right panel, due to the large displacement in the case of higher excitation energy. The bond length of chlorine is oscillating around a maximum at 5.9 a_0 with no significant deviation with time, like in the excitation at higher initial energy. To extract the vibrational frequencies, first the data was normalized to the deviation from the mean value and then a Fourier transformation was performed.

The zone boundary phonon, which could be attributed to the long living phonon mode observed in the experimental pump probe spectrum, see Fig. 1.8, has a frequency of 2.0 THz, according to a vibrational period of 500 fs. Fig. 6.27 shows the Fourier transformed data up to 1 ps. Longer vibrational periods exist, compare for example the displacements of the window atoms from Fig. 6.26, indicating a coupling between window and collision atoms, but they are not in the range interesting for the detection of the long living phonon mode.
There is one vibrational period of 286 fs, which appears for each group of atoms. Then, most interestingly, another period is found with 444 fs, which seems to reflect a coupling between belt and phonon atoms. Independent from the excitation energy, belt and phonon atoms seemed to be coupled, showing exactly the same vibrational period for simulations $>$ 4 ps. The frequencies do not fit the experimental data, but are inside a reasonable variation. For a determination

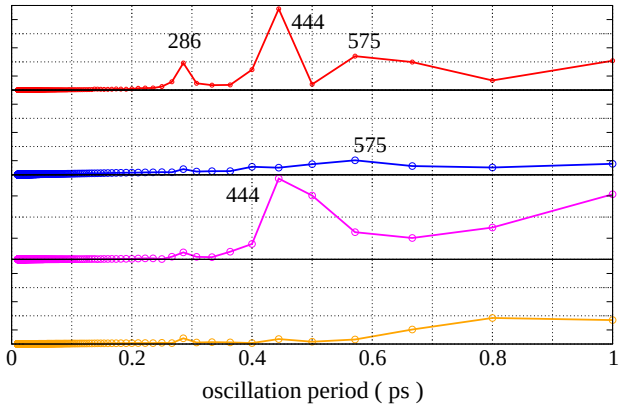

Figure 6.27: *Vibrational periods of belt, window, phonon and collision atoms (from top to bottom), calculated by FFT from excitation at 4.5* a_0

of the surviving phonon mode, a normal mode analysis has to be performed. Projection of the modes found after B-state excitation should then allow the identification of this special mode. From the classical dynamics simulations performed here, only evidence is given for a coupling between the belt and phonon atoms, which can be regarded as spanning perpendicular rectangles with the same center of mass, see Fig. 6.28. There is some evidence that the phonon atoms will be excited along with the promotion of chlorine from the ground to the B-state, but even for very low excitation energies a motion of the belt atoms will be initiated.

Concluding, even though from the simulations performed here the surviving phonon mode observed in the experiment could not be associated reliably with one of the groups of atoms proposed by Apkarian or Schwentner, evidence could be found, that oscillations of both belt and phonon atoms are initialized by switching the molecular wavefunction. These oscillations are localized in the vicinity of the chromophore and are not dissipating under the conditions used here. The motions of these groups of atoms is coupled, independent from the excitation energy, the same as found in the experiment, and shows a oscillation period, which is in the range of 500 fs. Therefore, the simulations performed here give evidence that both

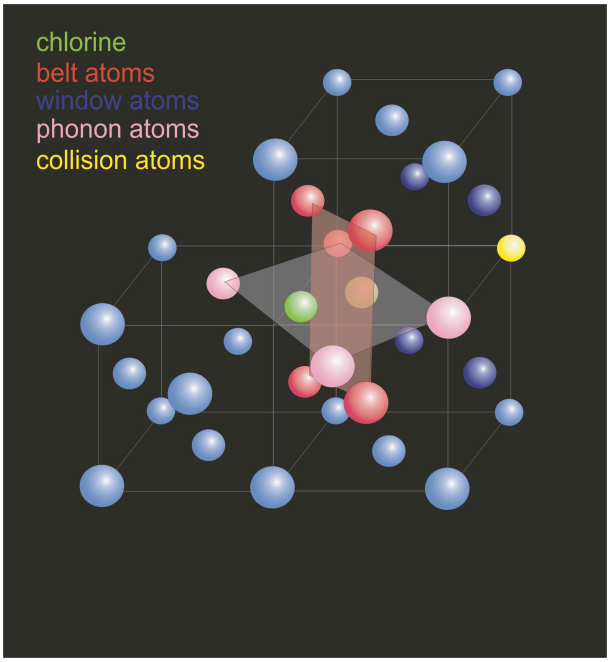

Figure 6.28: *Windows spanned by the belt and phonon atoms, respectively. The center of mass for both windows lies at the center of mass of the chromophore.*

groups of atoms are involved in the surviving phonon mode.

6.7.1.6 Vibrational Relaxation

The principal idea of simulating the energy loss for different initial energies lead to the revelation of different energy distribution schemes, dependent on the initial energy of the chromophore. The trend, that the energy loss is large for excitations above and significantly smaller for excitations below the dissociation limit. This trend is confirmed by the experimental results for Cl_2 in Ar, Fig. 1.14 and I_2 in Kr [66].

Determination of k_{rel}, the relaxation rate, are complicated by the events happening prior to the energy loss, resulting in an increase in the total energy of Cl_2. The discussion in the former sections shows the importance of the argon atoms in the surrounding of the chlorine molecule. The influence of different geometries of the system, especially for the low energy excitation and the increase of the total energy connected to this shows that there are more complicated processes than just simple relaxation by means of energy transfer. Therefore, due to the approximations used in the calculation of the energy loss, including 0 K as temperature and

the determination of energy loss in the first collision with different initial bond length, the calculated rate constants can only be compared qualitatively to the experimental data, which was shown in Fig. 1.14.
For the Cl-Cl distances discussed above a set of trajectories was calculated and weighted, but for a quantitative determination of the rate constants this number was not sufficient to give a good statistic. The discussion of the results achieved by representative trajectories can give insight in the principal effects and still the change in the slope of k_{rel} could be assigned to the different mechanisms of energy exchange with the lattice, see Fig. 6.29.

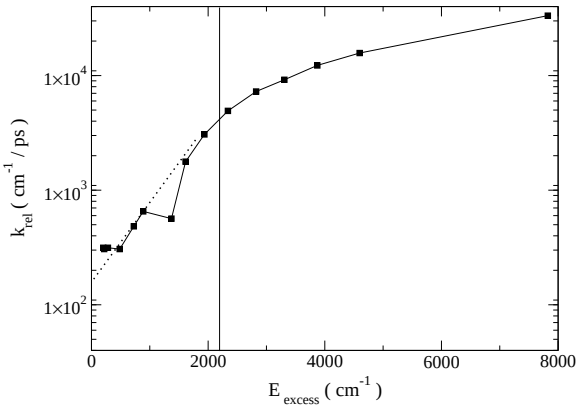

Figure 6.29: *Vibrational relaxation rate k_{rel} corresponding to different excitation energies. The gas phase dissociation limit is depicted by the solid line, the mean slope for excitations below the dissociation limit is depicted by the dashed line.*

For the excitations above the dissociation limit, Δ E can be connected to the first collision. Here the calculated values for the rate constant show a consistent behaviour, see Fig. 6.29. There is a steep slope for values of excess energy $>$2200, which represent the values above the dissociation limit, depicted by the straight line in Fig. 6.29. For lower values of excess energy the slope becomes much more flattened, until it becomes nearly zero for the lowest values. These values are for excitations into the bound part of the potential, where the interaction with the environment becomes very small. Calculation of k_{rel} in this energy range is complicated, since the determination of Δ E and Δ t is ambiguous, due to the preceding rise in total energy. In this sense the difference of energy from the maximum of the total energy to the following minimum was taken.

The calculated rate constants for vibrational relaxation of Cl_2 in Ar fit to the general behaviour observed in experiment and is consistent to the mechanism shown above. Compared to the experimental data, the values for the relaxation rate are 10 times larger than the experimental values. More calculations have to be performed to give more exact values for k_{rel}, to be compared directly to the experimental data.

6.8 Discussion

The system Cl_2 in Ar showed some interesting features. The orientation of the molecule in the lattice, occupying a double substitutional site with the molecular axis aligned in $\{110\}$ direction, see Fig. 1.3, lead to *perfect* caging. Therefore, the guest-host interaction especially concerning the collision atoms is very strong and photodissociation of the chromophore leads to a very effective momentum transfer from the chromophore to the lattice atoms, resulting in a shock wave. This can be compared to the system I_2 in Kr, due to the similar geometry of the system. Compared to the simulation of I_2/Kr [43], using a mass ratio of approximately 1.0, the same progression of the shock wave was found.
This shock wave lead to some problems concerning the size of the simulation box and for a better description of the system after excitation to the C-state a new box size was suggested. A box, which would allow the dynamics on the C-state or in the Franck-Condon region of the B-state should be extended mainly in the direction of the molecular axis, but has to include the next four layers of argon atoms. Especially for the excitations to the B-state it was found, that the other groups of atoms constituting the cage, the belt and window atoms, have some influence on the dynamics of the chromophore, which is not negligible. To reproduce the correct behaviour of these atoms, the next layers or cage shells have to be incorporated in the simulation.

The simulated excitation to the B-state with different bond length/excitation energies revealed the different channels for energy transfer. Excitation near the Franck-Condon region showed the same characteristics as for the excitation to the C-state. Again, shock waves were initialized and the loss of energy in the first collision event was significantly larger than found in the excitations at longer bond length/smaller excitation energy.
In the former case the energy or momentum was transferred to the collision

atoms, for excitations into the bound part of the B-state the energy loss was much smaller and now the energy loss is happening at times when the molecule is at its inner turning point, corresponding to the smallest values r_{Cl-Cl}. The slope of the relaxation rates calculated in this work reflects qualitatively the experimental results, with a more pronounced loss of energy above the dissociation limit, see Fig. 1.14, and was discussed for I_2 in Kr [66].
More quantitative information about the mechanisms leading to the decay rate k_{rel} can not be given here, due to the complex interaction between the chromophore and the other groups of atoms building the cage. The interaction with the cage atoms leads to various rearrangements in the geometry of the system, resulting in significant variations of the chromophore's total energy. However, an improved quantitative agreement is expected for simulations using a larger number of trajectories, the number used here is not sufficient to give good statistical results. Concluding, the underlying mechanism, which lead to a the general trend in the change of the experimentally observed relaxation rate, were enlightened. Two different channels for the energy dissipation were found for excitations above or below the potential well, including either the collision or the belt atoms, respectively.
In connection to these simulations it was shown, that for the excitations near to the potential minimum of the B-state the guest-host coupling decreases. This behaviour is also reflected in the experimental excitation spectrum Fig. 3.3 [20], where the vibrational states ≤ 7 show no significant phonon side band, but mainly the sharp zero phonon line, which can be described as the excitation of the vibrational level of the chromophore without a significant contribution from the surrounding environment. With respect to the observed long living phonon modes, evidence was given that not only one group of atoms could be responsible, but the coupled motion of belt and phonon atoms. Those two groups of atoms show an oscillation with a period of 444 fs, which is in rather good agreement to the experimentally found value of 500 fs.

State transitions were not included in this calculation, although from the pump-probe spectra Fig. 3.4 a spin-flip, a transition from the initially excited singlet to the triplet Π state has to be expected. Including quantum effect by the implementation of the surface hopping approach, for example, is necessary to give a more accurate description of the processes and will allow a direct comparison with the experimental results.